JCTC Journal of Chemical Theory and Computation

Rigorous Extraction of the Anisotropic Multispin Hamiltonian in Bimetallic Complexes from the Exact Electronic Hamiltonian

Rémi Maurice,*[,†,‡] Nathalie Guihéry,[†] Roland Bastardis,[§] and Coen de Graaf*[,‡,∥]

Laboratoire de Chimie et Physique Quantiques, IRSAMC/UMR5626, Université de Toulouse III, 118 route de Narbonne, F-31062 Toulouse Cédex 4, France, Departament de Química Física i Inorganica, Universitat Rovira i Virgili, Marcel·lí Domingo s/n, 43007 Tarragona, Spain, Laboratoire de Mathématiques, Physiques et Systemes, Université de Perpignan Via Domitia, 52 avenue Paul Alduy, 66860 Perpignan, France, and Institució Catalana de Recerca i Estudis Avançats (ICREA), Passeig Lluis Companys 23, 08010 Barcelona, Spain

Received July 8, 2009

Abstract: The magnetic anisotropy of the $[Ni_2(en)_4Cl_2]^{2+}$ (en = ethylenediamine) complex has been studied using wave function based computational schemes. The spin−orbit state interaction methodology provides accurate *ab initio* energies and wave functions that are used to interpret the anisotropy in bimetallic complexes. The extraction of the anisotropic spin Hamiltonian is performed using the effective Hamiltonian theory. This procedure which has successfully been applied to mononuclear complexes enables one to solve the weak exchange limit. It is shown that the standard coupled spin Hamiltonian only describes a part of the anisotropy of the molecule. Important higher order terms such as the biquadratic anisotropic exchange should be included in the model for an appropriate description of the anisotropy.

1. Introduction

The discovery of the unusual magnetic relaxation properties of the Mn_{12}-acetate cluster[1] triggered important research activity to find other molecule-based materials with similar magnetic properties. The interaction between different research areas in physics and chemistry proved to be a fruitful strategy in the design of new polynuclear species and the understanding of its peculiar magnetic properties.[2−7]

The basic requirements for systems to behave as single-molecule magnets (SMMs) are a high spin ground state of spin moment S and a sizable axial anisotropy characterized by an easy axis of magnetization and hence a negative zero-field splitting (ZFS) parameter D. These two factors lead to an energy barrier of $|D|\cdot S^2$ between the two states of opposite magnetization ($+M_s$ and $-M_s$). The presence of in-plane anisotropy leads to quantum tunneling effects which, on one hand, will speed the magnetization relaxation but, on the other hand, also introduce the possibility to study fundamental quantum phenomena such as coherence and interference effects. A detailed control over the anisotropy parameters would certainly be helpful in the development of new materials with higher energy barrier and higher blocking temperatures. Molecules with high nuclearities and/or high spin moments have been synthesized through an at least partially rational design.[8−11] Information about the anisotropy parameters D and E can be obtained from different experimental techniques, among which electron paramagnetic resonance (EPR) is particularly relevant.[12,13]

Theory also plays an important role in the description of the properties of SMMs. In the first place, theory provides important feedback to experiment by the interpretation of experimental data using model Hamiltonians.[14−18] Basically, there are two approaches to describe the magnetic phenomena in polynuclear systems: (1) the coupled spin Hamiltonian[19]

* Corresponding author phone: +33561556488; e-mail: rmaurice@irsamc.ups-tlse.fr (R.M.).

† Université de Toulouse III.

‡ Universitat Rovira i Virgili.

§ Université de Perpignan Via Domitia.

∥ Institució Catalana de Recerca i Estudis Avançats (ICREA).

10.1021/ct900473u
Published on Web 12/23/2009

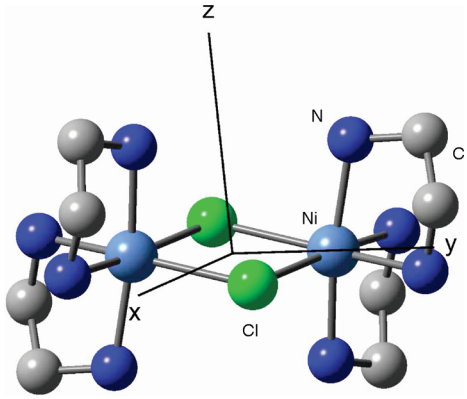

Figure 1. Ball and stick representation of $[Ni_2(en)_4Cl_2]^{2+}$. Hydrogen atoms are omitted for clarity. The magnetic axes are shown. The angle between the magnetic *z* axis and the normal of the Ni−(Cl_2)−Ni plane is 12°.

and (2) the giant spin Hamiltonian.[12] In the first model, the anisotropy of the molecule is obtained as resulting from the local anisotropies of the metal ions and the anisotropies of their interactions. In the giant spin approach, this information is lost and only the total spin of the ground state of the molecule is considered.

A second, more computational aspect of theory is the ability to derive magnetostructural correlations. This has a long-standing history in isotropically coupled magnetic centers, but recently the field has been extended to anisotropic spin moments.[20,21] Many of the computational studies of magnetic anisotropy are based on density functional theory.[20−26] The anisotropy is accounted for by a perturbational estimate of the effect of spin−orbit coupling on the lowest spin-free states.[23,24] Alternatively, a computational approach based on the *N*-electron wave function can be applied to study anisotropic effects in molecular magnetic systems, where the anisotropy can be addressed by perturbation theory[27] or variationally.[28−33]

Here, we present the *ab initio* description of the magnetic anisotropy in a bimetallic complex as a first step toward the theoretical study of anisotropy in larger, more interesting systems. The full *ab initio* description of the Mn_{12}-acetate complex is out of reach, but important information may be derived from bimetallic fragments that eventually can be extrapolated to polynuclear systems. The objective of our study is to validate and extract the multispin Hamiltonian to describe magnetic anisotropy, in particular in the weak exchange limit, i.e., for a weak isotropic exchange between the magnetic ions. For this purpose, a newly proposed procedure[34] based on the effective Hamiltonian theory is used to determine all the matrix elements of the effective Hamiltonian derived from the *ab initio* energies and wave functions and to consecutively extract all the spin operators that must be incorporated in the model Hamiltonian to reproduce at best the *ab initio* results. This methodology is applied to the $[Ni_2(en)_4Cl_2]^{2+}$ complex, shown in Figure 1.

Recently, high-field EPR data were published on this bimetallic Ni^{2+} complex.[35] These data were interpreted in terms of the coupled spin model, and values were given for the isotropic and axial anisotropic exchange interactions, in addition to the single-ion axial anisotropy parameter. The relatively small number of atoms makes this complex the ideal candidate for a detailed *ab initio* exploration of the electronic structure including spin−orbit interactions.

The paper is divided in three major parts. The first part describes the computational strategy that we apply to obtain the *ab initio* energies and wave functions of the lowest electronic states including spin−orbit coupling (see the following section). In the second part of the paper, we extract the parameters of the standard coupled spin Hamiltonian including both axial and rhombic anisotropy (see section 3). Finally, the validity and physical content of the coupled spin Hamiltonian are analyzed (see section 4).

2. Ab Initio Treatment of $[Ni_2(en)_4Cl_2]^{2+}$

Spin−orbit effects are accounted for variationally by the spin−orbit state interaction (SO-SI) method introduced by Malmqvist and co-workers[28,29] and implemented in Molcas 7.[36] In this method, a spin−orbit interaction matrix is constructed using the CASSCF *N*-electron wave functions of the ground state and a collection of excited states as basis functions. Thus, the SO-SI scheme requires not only an accurate description of the ground state but also of the lowest lying excited states. Actually, in order to introduce dynamic correlation, the CASSCF energies on the diagonal elements of the spin−orbit state interacting matrix are replaced by energies obtained at a high level of correlation such as CASPT2 or Difference Dedicated Configuration Interaction (DDCI). This procedure presents several degrees of freedom which were previously studied in monometallic complexes[34] and provides accurate anisotropic parameters.

Difference Dedicated Configuration Interaction (DDCI) is one of the most accurate methods to determine relative energies of electronic states with important multiconfigurational character. DDCI involves a two-step procedure consisting of treating the nondynamical electron correlation effects in a small reference space, and subsequently includes dynamical correlation by CI calculations. The CI space is spanned by all single and double electron replacements with respect to the reference wave function except for the excitations that promote two electrons from the inactive orbitals into the virtual ones.[37] Although DDCI has been applied mainly to the calculation of energy differences between states with a common electronic configuration (i.e., the energy differences involved in magnetic coupling problems),[38−47] the method has also been successful in spectroscopic problems.[48−50] The bottleneck of the method is the size of the CI space, which is determined to a large extent by the size of the reference space. For the full computational characterization of the ground and first excited states of the Ni-dimer, it is necessary to construct a reference space that contains the 10 Ni-3d orbitals and the 16 electrons occupying these orbitals. This reference space leads to intractable CI spaces even when applying the DDCI selection rules.

Alternatively, dynamical electron correlation effects can be estimated perturbatively. The CASPT2 implementation of multiconfigurational second-order perturbation theory[51] may rival in precision with DDCI but is applicable to larger systems. The method has, however, a major drawback.

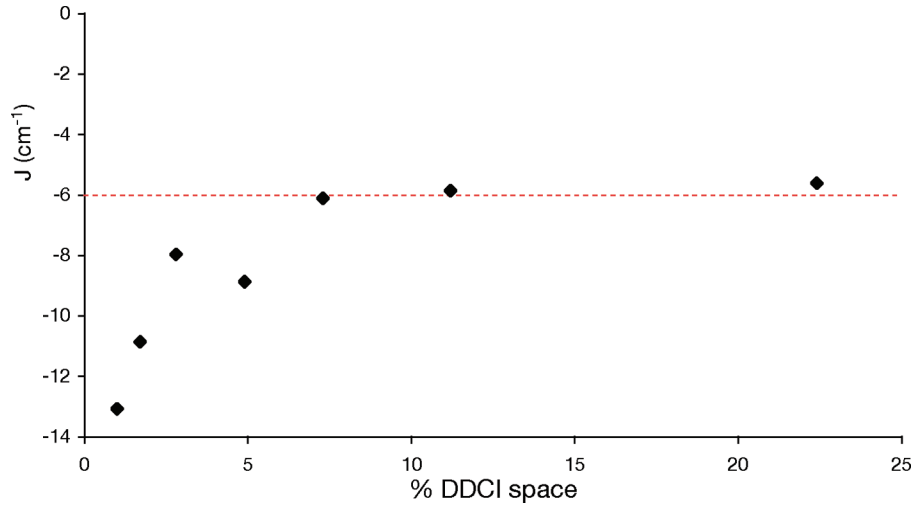

Figure 2. Magnetic coupling J (in cm^{-1}) as a function of the percentage of the space on which is performed the DDCI calculation.

Recently, it has been shown that CASPT2 cannot be applied to estimate magnetic coupling strengths for weakly coupled transition metals in bimetallic complexes.[52] Therefore, we adopted a two-step strategy to determine the spectrum of the Ni-dimer to take profit of the advantages of both methods. The relative energies of the lowest singlet, triplet, and quintet states, which arise from the magnetic coupling of the $S = 1$ spin moments on the Ni^{2+} ions, are calculated with DDCI, and the rest of the spectrum is calculated with CASPT2. Indeed, while a high precision is needed for these lowest states from which the spin Hamiltonian will be extracted, the CASPT2 precision is sufficient on the other excited states.[34] However, in order to ensure that the numerical errors have no consequences on the further qualitative conclusions, the results obtained using the CASSCF energies will be given for comparison.

2.1. Determination of the Isotropic *J*. The most common definition of the Heisenberg Hamiltonian in the field of magnetic anisotropy related to SMM is $\hat{H} = +J\hat{S}_i \cdot \hat{S}_j$, implying that $J > 0$ parametrizes antiferromagnetic coupling and $J < 0$ describes the ferromagnetic situation. The symmetry point group of $[Ni_2(en)_4Cl_2]^{2+}$ is C_i. This low symmetry makes the application of DDCI cumbersome. A straightforward procedure to reduce the computational cost of the DDCI calculation is to freeze the molecular orbitals (both occupied and virtual) that are less important for the energy difference between singlet, triplet, and quintet. A selection criterion based on orbital energies does not lead to a rapid convergence of the calculated J-values with the size of the MO space. A much better way to order the orbitals by increasing importance is obtained after the unitary transformation of the natural orbitals to so-called dedicated orbitals.[53] These orbitals are obtained by the diagonalization of the difference density matrix ρ_{diff}. For $[Ni_2(en)_4Cl_2]^{2+}$, the magnetic coupling involves three states, and the difference density matrix can be defined in several ways, which give practically the same results. Here we have chosen $\rho_{diff} = (\rho_Q - \rho_T) + (\rho_Q - \rho_S)$, where ρ is a density matrix and indexes Q, T, S refer to the low-lying quintet, triplet, and singlet spin−orbit free states, respectively. This reduction makes possible the DDCI calculation of the complex in the unsymmetrized, experimental geometry. Figure 2 shows how J varies with the size of the CI space which depends on the number of occupied and virtual MOs considered in the generation of the CI space. For severe truncations, we observe large oscillations, but the magnetic coupling J converges rapidly to a value around -6 cm^{-1}. One may notice that the CASSCF value is -2.2 cm^{-1}. Since the angle $\widehat{NiLNi}$ (where L is a Cl^- ion) is close to 90°, the delocalization between the Ni ions is expected to be weak between the $d_{x^2-y^2}$ orbitals, and weak as well between the d_{z^2} orbitals due to their small overlap. As a consequence, either a weakly antiferromagnetic or a ferromagnetic value of J was expected. The enhancement of ferromagnetism with electron correlation shows that the spin polarization favors the highest spin states in this system.

Table 1. IDDCI Magnetic Coupling Parameter (in cm^{-1}) for $[Ni_2(NH_3)_8Cl_2]^{2+}$

method	iteration	J(Q−T)	J(T−S)
IDDCI	1	−2.00	−2.13
	2	−3.30	−3.37
	3	−4.44	−4.49
	4	−5.22	−5.29
	5	−5.70	−5.77
	6	−5.99	−6.06

A second strategy to reduce the length of the CI expansion is to symmetrize the molecule and replace the ethylenediamine external ligands by simpler model ligands. The symmetrization to C_{2h} symmetry does not imply large displacements; especially, the angles and distances in the central Ni_2Cl_2 unit remain practically unchanged. Furthermore, the effect of the external ligands on the magnetic coupling parameter has been proven to be weak as long as the nature of the atom coordinating the metal remains the same.[54] Results of the iterative DDCI procedure on this $[Ni_2Cl_2(NH_3)_8]^{2+}$ model complex are reflected in Table 1. This process optimizes at each iteration a new set of MOs by diagonalizing the average density matrix $\rho_{avg} = \rho_Q + \rho_T + \rho_S$. We adopted this strategy to make the results independent of the starting orbital set and to remove the largest part of the basis set dependency.[55] To check the importance of

Table 2. SO-SI Energies (cm^{-1}) and Weight of the Different $|S, M_S\rangle$ Functions in the Low-Lying Spin Free Quintet, Triplet, and Singlet States Calculated in the CASSCF Space[a]

state	energy	$\|2, -2\rangle$	$\|2, -1\rangle$	$\|2, 0\rangle$	$\|2, 1\rangle$	$\|2, 2\rangle$	$\|1, -1\rangle$	$\|1, 0\rangle$	$\|1, 1\rangle$	$\|0, 0\rangle$
Ψ_1	0.000	0.41	0.00	0.09	0.00	0.41	0.00	0.00	0.00	0.06
Ψ_2	1.668	0.49	0.00	0.00	0.00	0.49	0.00	0.00	0.00	0.00
Ψ_3	8.752	0.00	0.49	0.00	0.49	0.00	0.00	0.00	0.00	0.00
Ψ_4	10.090	0.07	0.00	0.64	0.00	0.07	0.00	0.00	0.00	0.18
Ψ_5	12.014	0.00	0.00	0.00	0.00	0.00	0.00	0.97	0.00	0.00
Ψ_6	12.729	0.00	0.49	0.00	0.49	0.00	0.00	0.00	0.00	0.00
Ψ_7	19.719	0.00	0.00	0.00	0.00	0.00	0.49	0.00	0.49	0.00
Ψ_8	23.908	0.00	0.00	0.00	0.00	0.00	0.49	0.00	0.49	0.00
Ψ_9	29.498	0.00	0.00	0.24	0.00	0.00	0.00	0.00	0.00	0.74

[a] Ψ_1, Ψ_6, and Ψ_7 contain the $|S, -M_S\rangle + |S, M_S\rangle$ combination. Ψ_2, Ψ_3, and Ψ_8 contain the $|S, -M_S\rangle - |S, M_S\rangle$ combination.

the isotropic deviations from the expected Heisenberg splitting of the lowest energy levels, we calculated J from the energy difference of the singlet and triplet state ($J = E_T - E_S$) and from the triplet−quintet energy difference [($J = (1)/(2)(E_Q - E_T)$].

The results in Table 1 show that the DDCI energies follow almost perfectly the expected energy spacings (Heisenberg behavior), at difference with other Ni-dimers studied previously, which showed deviations up to 5% with respect to the Landé spacing.[56] The DDCI result converges in six iterations with respect to the shape of the natural orbitals to a J-value that is in perfect agreement with the result obtained with dedicated orbitals in the real complex.

2.2. Calculation of the Excited States. The singlet, triplet, and quintet states considered so far do not interact directly through spin−orbit coupling. The degeneracy of the M_S sublevels of these states is only lifted through the interaction with other excited states presenting a different spatial configuration. Previous studies on mononuclear Ni(II) complexes showed that the major effect on the spin−orbit splitting comes from the interaction between the ground state ($^3A_{2g}$ in the notation of the octahedral symmetry group) and the first excited triplet states ($^3T_{2g}$), which involves a single excitation of an electron from the t_{2g} to the e_g orbitals.[12,34] The next excited triplet state ($^3T_{1g}$) lies higher in energy and has a smaller interaction with the ground state because of the strong bielectronic excited character of this state. Extrapolating these findings to the Ni(II) dimer, we calculated the energies and wave functions of all 18 states that arise from the local $^3A_{2g} \rightarrow {}^3T_{2g}$ excitations.

State-averaged CASSCF calculations were performed for states with the same spin and spatial symmetry. The active space contains the 10 Ni-3d orbitals and 16 electrons, and dynamical correlation effects are estimated with CASPT2 for all electrons except those occupying the deep-core orbitals (1s, 2s, 2p, and 3s for Ni; 1s, 2s, and 2p for Cl; and 1s for C and N). The resulting spectrum shows three groups of six states at 0.92, 1.05, and ∼1.18 eV. Each group contains the singlet, triplet, or quintet spin coupled gerade and ungerade combination of the local $^3A_{2g} \rightarrow {}^3T_{2g}$ excitation on the left or right Ni(II) ion. The states arising from the next local triplet excitation start at 1.76 eV above the ground state and have not been considered in the determination of the spin−orbit resolved low-energy spectrum.

2.3. Effect of Spin−Orbit Coupling. Before analyzing the SO-SI results, it is preferable to make a proper choice of the coordinate frame. Although the energies are of course independent of the axes, the expression of the wave function of the spin−orbit states is strongly influenced by this choice and the interpretation of the results may be severely hindered if the principal magnetic axis does not coincide with the z-axis of the coordinate frame. Following the procedure described in the study of the monometallic Ni(II) complexes,[34] we extracted the magnetic axes of the molecule. In both monometallic and polymetallic complexes the tensor which is diagonalized (in order to extract the magnetic axes frame) only describes the ground state. In the considered case, the tensor has therefore been extracted using a giant spin Hamiltonian (**S**.**D**.**S**) describing only the quintet ground state. The proper magnetic axes frame is shown in Figure 1.

Spin−orbit coupling splits the lowest singlet, triplet, and quintet states in nine states. The weights of the $|S, M_S\rangle$ functions on which will be built the model anisotropic spin Hamiltonian in the wave functions of these states are given in Table 2. It can be noticed that the sum of these weights is close to 1 in each state, showing that this model space is appropriate; i.e., it contains the essential physics of the problem. The spectrum width (approximatively 30 cm^{-1}) is significantly increased by the spin−orbit coupling (spin−orbit free width = $3|J| = 18\ cm^{-1}$). At the CASSCF level $|J|$ is much smaller. The width of the spin−orbit spectrum is 19 cm^{-1} which is still larger than the CASSCF spin−orbit free spectrum ($3|J| = 7\ cm^{-1}$). This is a first indication of the importance of spin−orbit interactions and so of the magnetic anisotropy of this molecule. The axes frame almost coincides with the magnetic anisotropy axes frame, since the calculated wave functions show really small mixing of determinants that can interact due to the mismatch of the coordinate frame and the magnetic axes. Furthermore, we observe that the singlet and quintet strongly mix leading to a strong stabilization of the state dominated by the $|2, 0\rangle$ determinant and that the energetic ordering of the states is not strictly the one that is expected in the strong exchange limit ($J \gg D, E$); the $|1, 0\rangle$ has a lower energy than the $|2, -1\rangle + |2, 1\rangle$ state. One should notice that the molecule shows not only axial anisotropy but also important rhombic anisotropy. The states that are dominated by the $|S, M_S\rangle$ and $|S, -M_S\rangle$ determinants are not degenerate as would be expected in the case of pure axial anisotropy.

3. Parameter Extraction of the Standard Model Hamiltonian

The interpretation of the low-energy physics of bimetallic complexes with magnetic anisotropy is usually based on the following phenomenological model Hamiltonian:[57,58]

$$\hat{H} = J\hat{S}_a \cdot \hat{S}_b + \hat{S}_a\bar{\bar{D}}_a\hat{S}_a + \hat{S}_b\bar{\bar{D}}_b\hat{S}_b + \hat{S}_a\bar{\bar{D}}_{ab}\hat{S}_b + \bar{d}_{ab}\hat{S}_a \times \hat{S}_b \quad (1)$$

The first term describes the isotropic Heisenberg magnetic coupling of the local spin moments. The second and third terms account for the local single-ion anisotropies. The fourth term introduces a symmetric anisotropic exchange while the last term corresponds to the antisymmetric exchange. Since the studied complex is centrosymmetric, the antisymmetric exchange is strictly zero[59,60] (the local magnetic axes are colinear) and the $\mathbf{D}_a$ and $\mathbf{D}_b$ tensors are equal. Let us call D_a and E_a, respectively, the axial and rhombic anisotropy parameters of the local anisotropy tensors and D_{ab} and E_{ab} respectively, the axial and rhombic parameters of the symmetric anisotropic exchange tensors. As it will be shown later, the tensors $\mathbf{D}_a$, $\mathbf{D}_b$, and $\mathbf{D}_{ab}$ are diagonal in the same coordinate frame.

Several extractions can be performed from a given spectrum. The next paragraphs will compare different extractions and discuss their ability to reproduce the calculated spectrum.

First, we parametrize the model Hamiltonian in the strong exchange limit using the expressions shown in Figure 3,[58,61] as it is usually done. One should however note that the *ab initio* results show a significant spin mixing between the singlet and the quintet components which is not accounted for by the strong exchange extraction. To get reliable parameters, the extraction is performed using only those states which are not affected by the spin mixing. Indeed, an extraction performed by optimizing the parameters in order to reproduce at best all the states of the spectrum would lead to nonphysically grounded parameters. Taking into account only axial anisotropies, $D_a = -9.43$ cm^{-1} and $D_{ab} = 0.36$ cm^{-1}. These parameters lead to the spectrum shown in the first column of Figure 4. To estimate the quality of the model spectrum, a mean percentage of error δ is defined as follows:

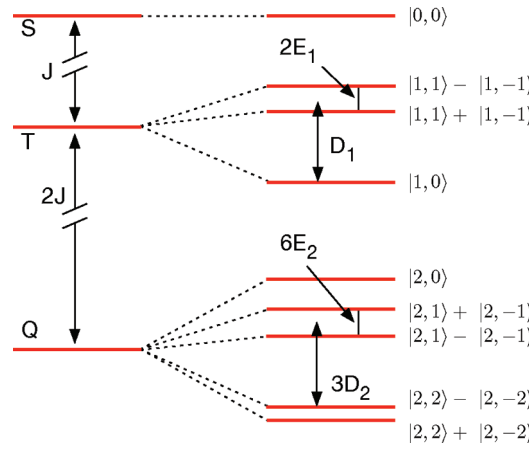

Figure 3. Energy levels of the quintet, triplet, and singlet states under the influence of spin−orbit coupling in the strong exchange limit: $D_1 = -D_a + D_{ab}$; $3D_2 = D_a + D_{ab}$; $E_1 = -E_a + E_{ab}$; $3E_2 = E_a + E_{ab}$.

$$\delta = \frac{\sum_i^N |E_i^{abinitio} - E_i^{model}|}{N \times \Delta E^{abinitio}} \times 100 \quad (2)$$

where N is the number of calulated roots, $\Delta E^{abinitio} = 29.498$ cm^{-1} is the *ab initio* spectrum width, and $E_i^{abinitio}$ and E_i^{model} are, respectively, the *ab initio* and model energies.

For the strong exchange limit with axial terms only, δ is as large as 7.2%. Adding rhombic anisotropy improves the

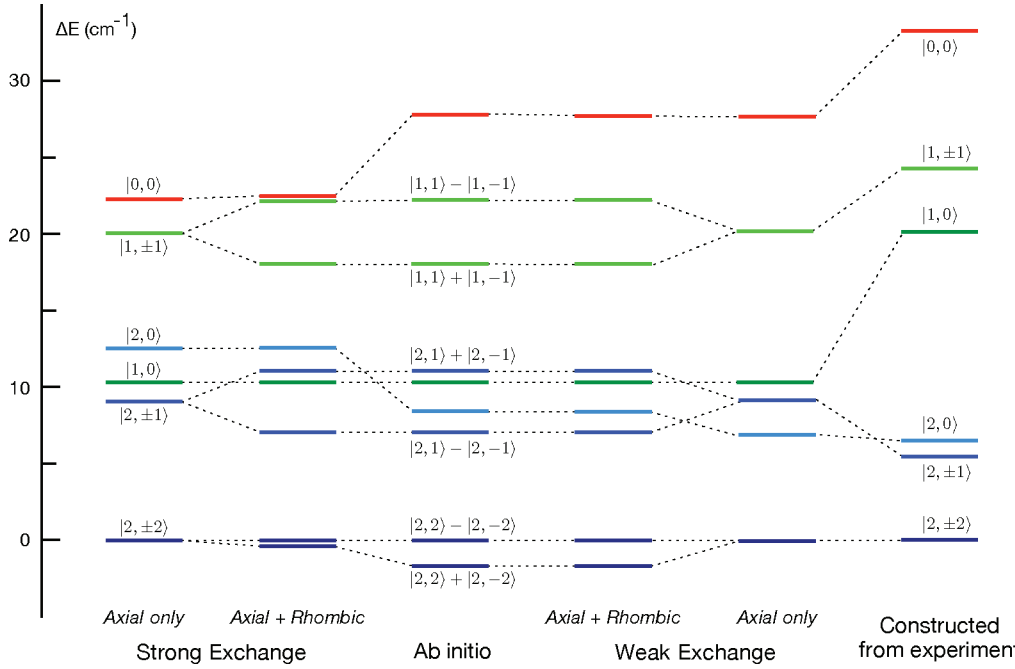

Figure 4. Comparison of the *ab initio* spectrum and model spectra obtained using different parametrizations.

model spectrum (second column, $\delta = 3.1\%$) and results in $E_a = -2.04$ cm^{-1} and $E_{ab} = 0.03$ cm^{-1}. The three states $|0, 0\rangle$, $|2, 0\rangle$, and $|2, 2\rangle + |2, -2\rangle$ which are strongly affected by the spin mixing between the singlet and the quintet are still poorly resolved by the model Hamiltonian in the strong exchange limit. At the CASSCF level, the anisotropic extracted parameters are of the same order of magnitude ($D_a = -7.07$ cm^{-1}, $D_{ab} = 0.30$ cm^{-1}, $E_a = 0.96$ cm^{-1}, and $E_{ab} = -0.39$ cm^{-1}) while $J = -2.60$ cm^{-1} is underestimated.

To further improve the representation of the *ab initio* spectrum by the model Hamiltanian, we follow the strategy outlined by Boča for the weak exchange limit, but never put to practice to the best of our knowledge. First, we determine analytically all model Hamiltonian matrix elements in the basis of the uncoupled $|M_{S_a}, M_{S_b}\rangle$ determinants (see Table 3). This 9×9 matrix is then transformed to the coupled $|S, M_S\rangle$ basis with the appropriate Clebsch−Gordan coefficients, and the five parameters of the model Hamiltonian can be determined by fitting the expressions of the eigenvalues of this Hamiltonian to the *ab initio* energies listed in Table 2. The Hamiltonian matrix in the coupled basis (given in Table 4) can be transformed into 2 smaller matrices: a 3×3 matrix spanned by the $|2, 2\rangle + |2, -2\rangle$, $|2, 0\rangle$, and $|0, 0\rangle$ functions and a 6×6 matrix within the $S = 1$ subspace, the $|2, \pm1\rangle$ determinants and the $|2, 2\rangle - |2, -2\rangle$ combination. Using the eigenenergies of $\Psi_{2,3,5-8}$, the parameters of the model Hamiltonian can be extracted from the 6×6 submatrix of the complete model Hamiltonian. Since the eigenstates of the 6×6 submatrix are not affected by the spin mixing, the parameters are practically identical to those extracted from the strong exchange limit. Nevertheless, in the weak exchange approach the three states affected by the spin mixing (see Figure 4, columns 4 and 5) are well reproduced and the overall error is 1.7% when rhombic anisotropy is neglected and only 0.07% when axial and rhombic terms are included. It is interesting to note that the lift of degeneracy between the $|2, 2\rangle$ and $|2, -2\rangle$ components is only correctly reproduced in the last extraction. This quantity (which determines the tunnel splitting) is crucial to understand the magnetization relaxation of SMMs at low temperature.

We also constructed the spectrum from the parameters that were extracted from the high-field EPR measurements reported by Herchel and co-workers.[35] Again, we only included axial terms as no estimates for E_a and E_{ab} were given in the paper. Using the parameters extracted from experiment ($J = -9.66$ cm^{-1}, $D_a = -4.78$ cm^{-1}, and $D_{ab} = -0.64$ cm^{-1}), we obtain a spectrum which exhibits a much smaller spin-mixing than the *ab initio* spectrum.

In summary, the largest differences between the *ab initio* spectrum and the spectrum extracted from experimental data is the degeneracy of the $|S, \pm M_S\rangle$ states in the latter one due to the absence of extracted rhombic anisotropy and the largest spin mixing in the *ab initio* spectrum.

4. Validity of the Model Hamiltonian

4.1. Transferability of the Single-Ion Anisotropy. Although the model Hamiltonian of eq 1 perfectly fits the *ab*

Table 3. Matrix Elements of the Model Hamiltonian for Bimetallic Ni(II) Complexes with Magnetic Anisotropy in the Uncoupled $|M_{S_a}, M_{S_b}\rangle$ Basis

$\lvert M_{S_a}, M_{S_b}\rangle$	$\lvert-1, -1\rangle$	$\lvert-1, 0\rangle$	$\lvert0, -1\rangle$	$\lvert-1, 1\rangle$	$\lvert0, 0\rangle$	$\lvert1, -1\rangle$	$\lvert1, 0\rangle$	$\lvert0, 1\rangle$	$\lvert1, 1\rangle$
$\langle -1, -1\rvert$	$J + (2/3)(D_a + D_{ab})$	0	0	E_a	E_{ab}	E_a	0	0	0
$\langle -1, 0\rvert$	0	$-(1/3)D_a$	$J - (1/3)D_{ab}$	0	0	0	E_a	E_{ab}	0
$\langle 0, -1\rvert$	0	$J - (1/3)D_{ab}$	$-(1/3)D_a$	0	0	0	E_{ab}	E_a	0
$\langle -1, 1\rvert$	E_a	0	0	$-J + (2/3)(D_a - D_{ab})$	$J - (1/3)D_{ab}$	0	0	0	E_a
$\langle 0, 0\rvert$	E_{ab}	0	0	$J - (1/3)D_{ab}$	$-(4/3)D_a$	$J - (1/3)D_{ab}$	0	0	E_{ab}
$\langle 1, -1\rvert$	E_a	0	0	0	$J - (1/3)D_{ab}$	$-J + (2/3)(D_a - D_{ab})$	0	0	E_a
$\langle 1, 0\rvert$	0	E_a	E_{ab}	0	0	0	$-(1/3)D_a$	$J - (1/3)D_{ab}$	0
$\langle 0, 1\rvert$	0	E_{ab}	E_a	0	0	0	$J - (1/3)D_{ab}$	$-(1/3)D_a$	0
$\langle 1, 1\rvert$	0	0	0	E_a	E_{ab}	E_a	0	0	$J + (2/3)(D_a + D_{ab})$

Table 4. Matrix Elements of the Model Hamiltonian for Bimetallic Ni(II) Complexes with Magnetic Anisotropy in the Coupled $|S, M_S\rangle$ Basis

$\|S, M_S\rangle$	$\|2, -2\rangle$	$\|2, -1\rangle$	$\|2, 0\rangle$	$\|2, 1\rangle$	$\|2, 2\rangle$
$\langle 2, -2\|$	$J + (2/3)(D_a + D_{ab})$	0	$[\sqrt{(2/3)}](E_a + E_{ab})$	0	0
$\langle 2, -1\|$	0	$J - (1/3)(D_a + D_{ab})$	0	$E_a + E_{ab}$	0
$\langle 2, 0\|$	$[\sqrt{(2/3)}](E_a + E_{ab})$	0	$J - (2/3)(D_a + D_{ab})$	0	$[\sqrt{(2/3)}](E_a + E_{ab})$
$\langle 2, 1\|$	0	$E_a + E_{ab}$	0	$J - (1/3)(D_a + D_{ab})$	0
$\langle 2, 2\|$	0	0	$[\sqrt{(2/3)}](E_a + E_{ab})$	0	$J + (2/3)(D_a + D_{ab})$
$\langle 1, -1\|$	0	0	0	0	0
$\|1, 0\rangle$	0	0	0	0	0
$\|1, 1\rangle$	0	0	0	0	0
$\|0, 0\rangle$	$[2/(\sqrt{3})](E_a - E_{ab})$	0	$[(\sqrt{2})/3](2D_a - D_{ab})$	0	$[2/(\sqrt{3})](E_a - E_{ab})$
	$\|1, -1\rangle$	$\|1, 0\rangle$	$\|1, 1\rangle$	$\|0, 0\rangle$	
$\|2, -2\rangle$	0	0	0	$[2/(\sqrt{3})](E_a - E_{ab})$	
$\|2, -1\rangle$	0	0	0	0	
$\|2, 0\rangle$	0	0	0	$[(\sqrt{2})/3](2D_a - D_{ab})$	
$\|2, 1\rangle$	0	0	0	0	
$\|2, 2\rangle$	0	0	0	$[2/(\sqrt{3})](E_a - E_{ab})$	
$\|1, -1\rangle$	$-J - (1/3)(D_a - D_{ab})$	0	$-E_a - E_{ab}$	0	
$\|1, 0\rangle$	0	$-J + (2/3)(D_a - D_{ab})$	0	0	
$\|1, 1\rangle$	$-E_a - E_{ab}$	0	$-J - (1/3)(D_a - D_{ab})$	0	
$\|0, 0\rangle$	0	0	0	$-2J$	

Table 5. Single-Ion Anisotropy Parameters (cm^{-1}) Obtained for Different Representations of the Monomer Fragment[a]

	$Ni(en)_2Cl_2$	+AIMP	$+Zn^{2+}$	$[Ni_2(en)_4Cl_2]^{2+}$
D_a	−4.82	−6.11	−6.13	−9.43
E_a	1.32	1.33	1.34	2.04

[a] For convenience, the values of the complete bimetallic complex have been added in the last column.

initio spectrum, the single-ion anisotropy parameters D_a and E_a are not the same as those obtained in the monomer fragment (see below). The local $\mathbf{D}_a$ tensor is changed by the anisotropy of neighboring metallic centers in another way than that captured by the molecular anisotropy parameter D_{ab}.

To calculate the single ion anisotropy of the monomer, we constructed several models. The most crude representation is removing one side of the bimetallic complex to obtain the $Ni(en)_2Cl_2$ monomer. A refined model is obtained by replacing one of the Ni ions with an *ab initio* model potential[62] or a closed-shell (and hence isotropic) Zn^{2+}ion. The atoms of the two remaining ethylenediamine groups are replaced with LoProp atomic charges[63] to reproduce the electrostatic environment of the real complex. The anisotropy parameters listed in Table 5 are obtained from CAS(8,5)SCF calculations using CASPT2 energies and a SO-SI space that contains the lowest four triplet states of the monomer. These are the computational parameters used in the dimer translated to the monomer case.

The two more refined models show identical results, and we observe that the single-ion anisotropy calculated in the monomer is between 30% and 50% smaller than the D_a parameter of the dimer. Two hypotheses may be formulated: (1) Delocalization effects between the metal ions are not strictly identical in the embedded monomer (no delocalization), the dimer involving a Zn^{2+} ion (small delocalization between the Ni $^{2+}$ and the closed shell Zn^{2+}), and the real dimer (more effective delocalization between the two Ni^{2+} ions). As a consequence, the resulting magnetic orbitals can be slightly different in the several calculations as well as the spin−orbit coupling involving these orbitals. (2) This could indicate a problem with the transferability of the single-ion anisotropy from monomers to polymeric systems, and the D_a parameter would not strictly parametrize the isolated single-ion anisotropy. In other words, the energy separations of the spin−orbit states would be partly caused by interactions that are present in the all electron Hamiltonian (i.e., in the *ab initio* results) but not included in the model Hamiltonian (eq 1).

4.2. Comparison with the Effective Hamiltonian. A rigorous check on the validity of the model Hamiltonian can be obtained by comparing it with an effective Hamiltonian spanned in the same basis. The effective Hamiltonian theory[64−68] is the bridge between the accurate *ab initio* results, which are difficult to interpret, and the easily understandable model Hamiltonians, which are in turn difficult to verify. By projection techniques, the *ab initio* information is reproduced in a small model space that hopefully contains all the essential physics. In a recent work on monometallic Ni(II) and 4-fold coordinated Co(II) complexes, we showed the validity of the standard Hamiltonian for zero-field splitting ($\hat{H} = \hat{S}\cdot\bar{\bar{D}}\cdot\hat{S}$) by comparing the model Hamiltonian to the corresponding effective Hamiltonian based on *ab initio* results.[34] Here, we follow the same procedure to check whether the model Hamiltonian of eq 1 contains all the important interactions for the magnetic anisotropy in bimetallic complexes.

In general, the effective Hamiltonian can be written as

$$\hat{H}^{\text{eff}} = \sum_i |\tilde{\Psi}_i\rangle E_i \langle\tilde{\Psi}_i| \tag{3}$$

where $\tilde{\Psi}_i$ are the orthogonalized projections on the model space of the exact (in practice, the *ab initio*) wave functions Ψ_i and E_i the energy eigenvalues. To ensure the Hermitic character of the effective Hamiltonian, we have applied an $S^{-1/2}$ orthonormalization of the projected vectors as proposed

by des Cloizeaux.[66] This procedure guarantees that the eigenvalues of the effective Hamiltonian are the same as for the all-electron Hamiltonian and that the corresponding eigenfunctions are the projections $\tilde{\Psi}_i$ of the eigenfunctions of the all-electron Hamiltonian onto the model space such that:

$$\hat{H}^{\text{eff}}|\tilde{\Psi}_i\rangle = E_i|\tilde{\Psi}_i\rangle \quad (4)$$

In any arbitrary frame, the off-diagonal elements of the $\mathbf{D}_a$, $\mathbf{D}_b$, and $\mathbf{D}_{ab}$ tensors are nonzero. The corresponding analytical expression of the coupled-spin Hamiltonian matrix is given in the Supporting Information. The values of the matrix elements of the effective Hamiltonian (given in Table 6) show that the local anisotropy axes coincide with the magnetic axes of the molecule (determined from the giant spin Hamiltonian). All matrix elements arising from off-diagonal terms in the D_a and D_{ab} tensors are almost zero between the components of the quintet state (for which the axis frame has been extracted) and negligible between the other states components (see Supporting Information). Since the optimal orbital sets for the quintet, the triplet, and the singlet spin−orbit free states are different, it is not mathematically possible to define a proper magnetic axes frame shared by all these states. Nevertheless, the smallness of the off-diagonal terms of all these tensors shows that a proper magnetic axes frame can reasonably be determined for the study of the coupled-spin Hamiltonian and that these tensors can be considered as being diagonal in this axes frame.

A closer inspection reveals important differences between the model Hamiltonian matrix and the effective Hamiltonian matrix. The most spectacular difference between the two matrices concerns the $\langle 1, -1|\hat{H}|-1, 1\rangle$ matrix element. These determinants do not interact through the model Hamiltonian (see also Table 3), but the effective Hamiltonian shows a large matrix element equal to 8.6 cm^{-1}. Furthermore, $\langle -1, 0|\hat{H}^{\text{eff}}|0, -1\rangle \neq \langle -1, 1|\hat{H}^{\text{eff}}|0, 0\rangle$, while the model Hamiltonian predicts equal interactions for these determinants. The same occurs for the matrix elements $\langle -1, -1|\hat{H}|1, -1\rangle$ and $\langle -1, 0|\hat{H}|1, 0\rangle$, and the matrix elements $\langle -1, -1|\hat{H}|0, 0\rangle$ and $\langle -1, 0|\hat{H}|0, 1\rangle$.

In order to check that these unexpected results are not due to an artifact of CASPT2, the effective Hamiltonian has been extracted from the CASSCF spectrum and wave functions (see Supporting Information). The form of the effective Hamiltonian is similar, exhibiting nonzero elements and either small or large elements at the same place in the matrix. In this case the $\langle 1, -1|\hat{H}| -1, 1\rangle$ matrix element is equal to 6.4 cm^{-1} and the observed deviations between the model and the effective Hamiltonians are similar.

To account for the largest interaction that emerges from the effective Hamiltonian, it is necessary to include fourth-order interactions in the model Hamiltonian. The $|-1, 1\rangle$ determinant is coupled to $|1, -1\rangle$ by the $\hat{S}_a^+\hat{S}_a^+\hat{S}_b^-\hat{S}_b^-$ operator. A new model Hamiltonian including such fourth-order terms can be defined as:

$$\hat{H} = J\hat{S}_a \cdot \hat{S}_b + \hat{S}_a\bar{\bar{D}}_a\hat{S}_a + \hat{S}_b\bar{\bar{D}}_b\hat{S}_b + \hat{S}_a\bar{\bar{D}}_{ab}\hat{S}_b + \vec{S}_a \otimes \vec{S}_a \cdot \mathbf{D}_{aabb} \cdot \vec{S}_b \otimes \vec{S}_b \quad (5)$$

Table 6. Numerical Matrix Elements of the Effective Hamiltonian in the Uncoupled $|M_{S_a}, M_{S_b}\rangle$ Basis in the Magnetic Axes Frame

H^{eff}	$\|-1, -1\rangle$	$\|-1, 0\rangle$	$\|0, -1\rangle$	$\|-1, 1\rangle$	$\|0, 0\rangle$	$\|1, -1\rangle$	$\|1, 0\rangle$	$\|0, 1\rangle$	$\|1, 1\rangle$
$\langle -1, -1\|$	1.670	−0.001 + 0.002i	−0.001 + 0.002i	−0.706 − 0.011i	2.686 + 0.011i	−0.706 − 0.011i	0.000	0.000	0.002
$\langle -1, 0\|$	−0.001 − 0.002i	16.278	−5.536	0.000	−0.010 + 0.035i	0.020 − 0.070i	2.042 + 0.013i	−0.053 − 0.012i	0.000
$\langle 0, -1\|$	−0.001 − 0.002i	−5.536	16.278	0.020 − 0.070i	−0.010 + 0.035i	0.000	−0.053 − 0.012i	2.042 + 0.013i	0.000
$\langle -1, 1\|$	−0.706 + 0.011i	0.000	0.020 + 0.070i	20.621	−1.309	8.599	−0.020 + 0.070i	0.000	−0.706 − 0.012i
$\langle 0, 0\|$	2.686 − 0.011i	−0.010 − 0.035i	−0.010 − 0.035i	−1.309	8.698	−1.309	0.010 − 0.035i	0.010 − 0.035i	2.686 + 0.011i
$\langle 1, -1\|$	−0.706 + 0.011i	0.020 + 0.070i	0.000	8.599	−1.309	20.621	0.000	−0.020 + 0.070i	−0.707 − 0.012i
$\langle 1, 0\|$	0.000	2.042 − 0.013i	−0.053 + 0.012i	−0.020 − 0.070i	0.010 + 0.035i	0.000	16.278	−5.536	0.001 − 0.002i
$\langle 0, 1\|$	0.000	−0.053 + 0.012i	2.042 − 0.013i	0.000	0.010 + 0.035i	−0.020 − 0.070i	−5.536	16.278	0.001 − 0.002i
$\langle 1, 1\|$	0.002	0.000	0.000	−0.707 + 0.012i	2.686 − 0.011i	−0.707 + 0.012i	0.001 + 0.002i	0.001 + 0.002i	1.670

where $\mathbf{D}_{aabb}$ is a fourth-order tensor, a 9 × 9 matrix, where $a, b = x, y, z$. The first two indices refer to site a, the other two to site b.

This new model Hamiltonian defined by the sum of the isotropic exchange, local and intersite anisotropy, and a term that describes the biquadratic anisotropic exchange significantly improves the comparison with the effective Hamiltonian. The $\langle -1, 1|H^{\text{eff}}|1, -1\rangle$ matrix elements appear in the new model Hamiltonian as the $(1/4)(D_{xxxx} + D_{yyyy}) + D_{xyxy} - (1/2)D_{xxyy}$ fourth-order in-plane interaction. This is, however, not the only improvement. The fourth-order term also contains operators such as $\hat{S}_a^+\hat{S}_a^+\hat{S}_b^z\hat{S}_b^z$ and $\hat{S}_a^+\hat{S}_a^z(\hat{S}_b^+\hat{S}_b^z + \hat{S}_b^z\hat{S}_b^+)$, which cause differential contributions for the other matrix elements that were found to be different in the effective Hamiltonian and equal in the standard model Hamiltonian. The complete matrix representation of the new model Hamiltonian perfectly reproduces the symmetry of the numerical effective Hamiltonian, and its expression in the magnetic axes frame can be found in the Supporting Information. At the CASSCF level the model and effective Hamiltonians are also in perfect agreement.

This new definition of the model Hamiltonian for magnetic anisotropy involves the parametrization of at least 14 interactions, namely the isotropic exchange coupling (J), the local anisotropy parameters D_a and E_a, the anisotropic exchange parameters D_{ab} and E_{ab}, and nine parameters that define the fourth-order tensor. Actually, the 81 elements reduce to just 15 nonzero elements in an appropriate coordinate frame and finally to nine differents parameters due to the symmetry of the system. Nevertheless, there are only nine states in the model space, and there is no direct way to derive analytical expressions for the parameters, not even using all the information in the effective Hamiltonian. In any case, it is not very convenient to work with so many parameters.

The above presented analysis leads to the conclusion that fourth-order anisotropic interactions are non-negligible in Ni(II) polymetallic systems, and that the rigorous extraction of the magnetic anisotropy parameters is not possible without introducing any further approximation. Although the definition of the spin Hamiltonian as a sum of isotropic, second-order anisotropic, and fourth-order anisotropic terms leads to a better understanding of the physics, it does not provide the tools to describe the phenomenon in a practical manner due to the large number of parameters.

5. Conclusions

The extraction of the magnetic anisotropy parameters in bimetallic complexes has been performed within the coupled Hamiltonian formalism. The local anisotropic spin moments are coupled by isotropic and anisotropic exchange interactions to describe the total magnetic behavior of the molecule. The most important conclusions obtained from both CASSCF and CASPT2 calculations can be summarized in the following paragraphs.

The standard coupled Hamiltonian gives an excellent fit of the *ab initio* spectrum. However, the comparison of the matrix representation of this Hamiltonian and the effective Hamiltonian constructed from the calculated energies and wave functions shows important discrepancies. Therefore, it is concluded that while the effective parameters of the standard Hamiltonian enable one to reproduce the spectrum, this Hamiltonian does not contain all the operators required to describe the physics of the anisotropic exchange.

A rigorous description of the magnetic anisotropy in $[Ni_2(en)_4Cl_2]^{2+}$ requires the use of fourth-order interactions. Test calculations on a bimetallic Co^{2+} complex show that sixth-order interactions appear in the effective Hamiltonian. Hence, the spin Hamiltonian should include spin operators up to order $2S_{\text{max}}$, in addition to the standard operators for local anisotropy, and isotropic and anisotropic exchange interactions. This Hamiltonian enables one to reproduce the matrix of the effective Hamiltonian extracted from the *ab initio* calculations.

In the giant spin approximation, the molecule is treated as an effective monometallic species with one (giant) spin for which the anisotropic properties can be determined. One important perspective will be the extraction of the giant spin Hamiltonian and the study of the effect of the coupled-spin fourth-order interactions in this formalism. Analytical relations between the multispin and giant spin Hamiltonian have to be found; this is the subject of ongoing research.

Acknowledgment. Financial support has been provided by the Spanish Ministry of Science and Innovation (Project CTQ2008-06644-C02-01), and the Generalitat de Catalunya (Project 2005SGR-00104 and *Xarxa d'R+D+I en Química Teorica i Computacional*, XRQTC). This work was supported by the French Centre National de la Recherche Scientique (CNRS), Université de Toulouse.

Supporting Information Available: Matrix elements of the standard coupled spin Hamiltonian in the $|M_{S_A}, M_{S_B}\rangle$ basis in an arbitrary coordinate frame, SO-SI spectrum of $[Ni_2(en)_4Cl_2]^{2+}$ as function of the isotropic exchange J, orthonormalized projections of the *ab initio* wave functions on the $|S, M_S\rangle$ model space, effective Hamiltonian in the $|S, M_S\rangle$ space, effective Hamiltonian in $|M_{S_A}, M_{S_B}\rangle$ basis obtained with the CASSCF spin-free energies on the diagonal of the spin−orbit matrix, and the coupled spin Hamiltonian matrix extended with fourth-order interaction in the magnetic axes frame. This material is available free of charge via the Internet at http://pubs.acs.org.

References

(1) Sessoli, R.; Gatteschi, D.; Caneschi, A.; Novak, M. A. *Nature* **1993**, *365*, 141.

(2) Gatteschi, D.; Sessoli, R. *Angew. Chem., Int. Ed.* **2003**, *42*, 269.

(3) Gatteschi, D.; Sessoli, R.; Villain, F. *Molecular Nanomagnets*; Oxford University Press: Oxford, 2006.

(4) Aromí, G.; Aubin, S. M. J.; Bolcar, M. A.; Christou, G.; Eppley, H. J.; Folting, K.; Hendrickson, D. N.; Huffman, J. C.; Squire, R. C.; Tsai, H.-L.; Wang, S.; Wemple, M. W. *Polyhedron* **1998**, *17*, 3005.

(5) Delfs, C.; Gatteschi, D.; Pardi, L.; Sessoli, R.; Wieghardt, K.; Hanke, D. *Inorg. Chem.* **1993**, *32*, 3099.

(6) Yang, E.-C.; Wernsdorfer, W.; Zakharov, L.; Karaki, Y.; Yamaguchi, A.; Isidro, R. M.; Lu, G. D.; Wilson, S.; Rheingold, A. L.; Ishimoto, H.; Hendrickson, D. N. *Inorg. Chem.* **2006**, *45*, 529.

(7) Milios, C. J.; Inglis, R.; Vinslava, A.; Bagai, R.; Wernsdorfer, W.; Parsons, S.; Perlepes, S. P.; Christou, G.; Brechin, E. K. *J. Am. Chem. Soc.* **2007**, *129*, 12505.

(8) Müller, A.; Das, S. K.; Talismanova, M. O.; Bögge, H; Kögerler, P.; Schmidtman, M.; Talismanov, S. S.; Luban, M.; Krickemeyer, E. *Angew. Chem., Int. Ed.* **2002**, *41*, 579.

(9) Tasiopoulos, A. J.; Vinslava, A.; Wernsdorfer, W.; Abboud, K. A.; Christou, G. *Angew. Chem., Int. Ed.* **2004**, *43*, 2117.

(10) Larionova, J.; Gross, M.; Pilkington, M.; Andres, H.; Stoeckli-Evans, H.; Güdel, H. U.; Decurtins, S. *Angew. Chem., Int. Ed.* **2000**, *39*, 1605.

(11) Oshio, H.; Hoshino, N.; Ito, T.; Nakano, M.; Renz, F.; Gütlich, P. *Angew. Chem., Int. Ed.* **2003**, *42*, 223.

(12) Abragam, A.; Bleany, B. *Electron Paramagnetic Resonance of Transition Ions*; Dover Publications: Dover, NY, 1986.

(13) Bencini, A.; Gatteschi, D. *EPR of Exchange Coupled Systems*; Springer-Verlag: Berlin, 1990.

(14) Barra, A.-L.; Gatteschi, D.; Sessoli, R. *Phys. Rev. B* **1997**, *56*, 8192.

(15) Moragues-Cánovas, M.; Helliwell, M.; Ricard, L.; Riviere, E.; Wernsdorfer, W.; Brechin, E.; Mallah, T. *Eur. J. Inorg. Chem.* **2004**, 2219.

(16) Duboc, C.; Phoeung, T.; Zein, S.; Pécaut, J.; Collomb, M.-N.; Neese, F. *Inorg. Chem.* **2007**, *46*, 4905.

(17) Piligkos, S.; Bill, E.; Collison, D.; McInnes, E. J. L.; Timco, G. A.; Weihe, H.; Winpenny, R. E. P.; Neese, F. *J. Am. Chem. Soc.* **2007**, *129*, 760.

(18) Chibotaru, L.; Ungur, L.; Aronica, C.; Elmoll, H.; Pilet, G.; Luneau, D. *J. Am. Chem. Soc.* **2008**, *130*, 12445.

(19) Borrás-Almenar, J. J.; Clemente-Juan, J. M.; Coronado, E.; Tsukerblatt, B. S. *Inorg. Chem.* **1999**, *38*, 6081.

(20) Ruiz, E.; Cirera, J.; Cano, J.; Alvarez, S.; Loose, C.; Kortus, J. *Chem. Commun.* **2008**, 52.

(21) Cirera, J.; Ruiz, E.; Alvarez, S.; Neese, F.; Kortus, J. *Chem. Eur. J.* **2009**, *15*, 4078.

(22) Park, K.; Pederson, M. R.; Richardson, S. L.; Aliaga-Alcalde, N.; Christou, G. *Phys. Rev. B* **2003**, *68*, 020405.

(23) Pederson, M. R.; Khanna, S. N. *Phys. Rev. B* **1999**, *60*, 9566.

(24) Kortus, J.; Hellberg, C. S.; Pederson, M. R. *Phys. Rev. Lett.* **2001**, *86*, 3400.

(25) Neese, F. *J. Chem. Phys.* **2007**, *127*, 164112.

(26) Ribas-Arino, J.; Baruah, T.; Pederson, M. R. *J. Chem. Phys.* **2005**, *123*, 044303.

(27) Neese, F. *J. Am. Chem. Soc.* **2006**, *128*, 10213.

(28) Malmqvist, P.-Å.; Roos, B. O. *Chem. Phys. Lett.* **1989**, *155*, 189.

(29) Malmqvist, P.-Å.; Roos, B. O.; Schimmelpfennig, B. *Chem. Phys. Lett.* **2002**, *357*, 230.

(30) Llusar, R.; Casarrubios, M.; Barandiarán, Z.; Seijo, L. *J. Chem. Phys.* **1996**, *105*, 5321.

(31) Webb, S. P.; Gordon, M. S. *J. Chem. Phys.* **1998**, *109*, 919.

(32) de Graaf, C.; Sousa, C. *Int. J. Quantum Chem.* **2006**, *106*, 2470.

(33) Chibotaru, L.; Ungur, L.; Soncini, A. *Angew. Chem., Int. Ed.* **2008**, *47*, 4126.

(34) Maurice, R.; Bastardis, R.; de Graaf, C.; Suaud, N.; Mallah, T.; Guihéry, N. *J. Chem. Theory Comput.* **2009**, *5*, 2977.

(35) Herchel, R.; Boča, R.; Krzystek, J.; Ozarowski, A.; Durán, M.; van Slageren, J. *J. Am. Chem. Soc.* **2007**, *129*, 10306.

(36) Karlström, G.; Lindh, R.; Malmqvist, P.-Å.; Roos, B. O.; Ryde, U.; Veryazov, V.; Widmark, P.-O.; Cossi, M.; Schimmelpfennig, B.; Neograd y, P.; Seijo, L. *Comput. Mater. Sci.* **2003**, *28*, 222.

(37) Miralles, J.; Daudey, J.-P.; Caballol, R. *Chem. Phys. Lett.* **1992**, *198*, 555.

(38) Broer, R; Maaskant, W. J. A. *Chem. Phys.* **1986**, *102*, 103.

(39) de Graaf, C.; Illas, F. *Phys. Rev. B* **2001**, *63*, 014404.

(40) Cabrero, J.; de Graaf, C.; Bordas, E.; Caballol, R.; Malrieu, J.-P. *Chem. Eur. J.* **2003**, *9*, 2307.

(41) Herebian, D.; Wieghardt, K.; Neese, F. *J. Am. Chem. Soc.* **2003**, *125*, 10997.

(42) Gellé, A.; Munzarová, M. L.; Lepetit, M. B.; Illas, F *Phys. Rev. B* **2003**, *68*, 125103.

(43) Neese, F. *J. Chem. Phys.* **2003**, *119*, 9428.

(44) Calzado, C. J.; Malrieu, J.-P. *Phys. Rev. B* **2004**, *69*, 094435.

(45) Bastardis, R.; Guihéry, N.; Suaud, N. *Phys. Rev. B* **2007**, *75*, 132403.

(46) Le Guennic, B.; Petit, S.; Chastanet, G.; Pilet, G.; Luneau, D.; Ben Amor, N.; Robert, V. *Inorg. Chem.* **2008**, *47*, 572.

(47) Barone, V.; Cacelli, I.; Ferrati, A.; Prampolini, G. *Phys. Chem. Chem. Phys.* **2009**, *11*, 3854.

(48) García, V. M.; Caballol, R.; Malrieu, J.-P. *J. Chem. Phys.* **1998**, *109*, 504.

(49) Cabrero, J.; Caballol, R.; Malrieu, J.-P. *Mol. Phys.* **2001**, *100*, 919.

(50) Rodríguez, E.; Reguero, M. *J. Phys. Chem. A* **2002**, *106*, 504.

(51) Andersson, K.; Malmqvist, P.-Å.; Roos, B. O. *J. Chem. Phys.* **1992**, *96*, 1218.

(52) Queralt, N.; Taratiel, D.; de Graaf, C.; Caballol, R.; Cimiraglia, R.; Angeli, C. *J. Comput. Chem.* **2008**, *29*, 994.

(53) Calzado, C. J.; Malrieu, J.-P.; Cabrero, J.; Caballol, R. *J. Phys. Chem. A* **2000**, *104*, 11636.

(54) Bordas, E.; Caballol, R.; de Graaf, C. *THEOCHEM* **2005**, *727*, 173.

(55) García, V. M.; Castell, O.; Caballol, R.; Malrieu, J.-P. *Chem. Phys. Lett.* **1995**, *238*, 222.

(56) Bastardis, R.; Guihéry, N.; de Graaf, C. *J. Chem. Phys.* **2008**, *129*, 104102.

(57) Kahn, O. *Molecular Magnetism*; VCH Publishers: New York, 1993; pp 135−143.

(58) Boča, R. *Theoretical Foundations of Molecular Magnetism*; Elsevier: Amsterdam, 1999; pp 642−680.

(59) Dzyaloshinsky, I. *J. Phys. Chem. Solids* **1958**, *4*, 241.

(60) Moriya, T. *Phys. Rev.* **1960**, *120*, 91.

(61) Boča, R. *Coord. Chem. Rev.* **2004**, *248*, 757.

(62) Barandiarán, Z.; Seijo, L. *J. Chem. Phys.* **1988**, *89*, 5739.

(63) Gagliardi, L.; Lindh, R.; Karlström, G. *J. Chem. Phys.* **2004**, *121*, 4494.

(64) Bloch, C. *Nucl. Phys.* **1958**, *6*, 329.

(65) Bloch, C.; Horowitz, J. *Nucl. Phys.* **1958**, *8*, 91.

(66) des Cloizeaux, J. *Nucl. Phys.* **1960**, *20*, 321.

(67) Malrieu, J.-P.; Durand, P.; Daudey, J.-P. *J. Phys. A: Math Gen.* **1985**, *18*, 809.

(68) Heully, J.-L.; Malrieu, J.-P. *Chem. Phys.* **2009**, *356*, 76.

CT900473U